1

Domain Decomposition Methods for Non-Symmetric Problems

Y. Achdou[1], C. Japhet[2], P. Le Tallec[3], F. Nataf[4], F. Rogier[5] & M. Vidrascu[6]

Introduction

The two algorithms presented below are especially fitted for non-symmetric elliptic problems. The model equation is the convection-diffusion equation:

$$\frac{\partial u}{\partial t} + \vec{a}.\nabla u - \nu \Delta u = f \tag{1}$$

This equation is important in itself in engineering or environnemental sciences for instance. It models the transport and diffusion of species (pollutant in air or water, electrons in semiconductor devices, ...) in a given flow (with velocity field $\vec{a}$) . It is also a key ingredient in Navier-Stokes equations. An implicit scheme in time will demand at each time step the solving of

$$\mathcal{L}(u) \equiv \frac{u}{\Delta t} + \vec{a}.\nabla u - \nu \Delta u = f \tag{2}$$

1 Insa Rennes, 20 Av. des Buttes de Coesmes, 35043 Rennes, France. yves.achdou@insa-rennes.fr
2 ONERA and CMAP, Ecole Polytechnique, 91128 Palaiseau, France. japhet@onera.fr
3 Universty of Paris IX, Ceremade, Paris, France, letallec@ceremade.dauphine.fr
4 address to whom correspondance should be sent: CMAP, Ecole Polytechnique, 91128 Palaiseau, France. nataf@cmapx.polytechnique.fr
5 ONERA-CERT, 2 av. Edouard Belin - BP 4025 - 31055 TOULOUSE CEDEX 4 - FRANCE , Francois.Rogier@cert.fr
6 INRIA Rocquencourt, domaine de Voluceau, BP105, 78153 Le Chesnay, France, Marina.Vidrascu@inria.fr
Eleventh International Conference on Domain Decomposition Methods
Editors Choi-Hong Lai, Petter E. Bjørstad, Mark Cross and Olof B. Widlund

The first algorithm is a preconditioner for the Schur formulation of domain decomposition problems. It is an extension of the well-known Neumann-Neumann preconditioner [BGLTV89] to non-symmetric problems. The second algorithm is an optimized Schwarz method. The Dirichlet boundary conditions on the interfaces are replaced by more general boundary conditions. The algorithm can then be used on non-overlapping (and/or overlapping) subdomains and has a fast convergence.

In this presentation, we emphasize the use of the Fourier transform on the continuous problem as a tool of analysis and design. Hence, we consider the simple geometry of the plane $\mathbf{R}^2$ divided into two or more vertical strips. This might seem inappropriate since Fourier analysis is essentially limited to constant coefficients operators and since computations are made on discretized problems and not on continuous models. Moreover, real life geometries are more complex. Variational settings or matrix analysis, for instance, do not have these limitations. Nevertheless, some ideas come up much more easily in the Fourier space and are then independent of the discretization scheme. Moreover, as we shall see, the methods that we propose are not limited to constant coefficient operators and can be used with various numerical schemes.

More precisely, in § 1 we study the Neumann-Neumann preconditioner when applied to a non-symmetric operator. We explain why it is not adapted. In the next section, we extend it to non-symmetric operators by modifying the Neumann boundary conditions. We shall also see how to write it by using a variational formulation for variable coefficients. Numerical results are shown to illustrate the efficiency of the preconditioner. We mention also the fact that it can be used in a FETI framework, see [FMR94].

In § 1, we turn to the classical Schwarz algorithm. We show that by changing the interface conditions, much better convergence rates can be reached. In § 1, we present an optimization procedure for choosing efficient and easy to implement interface conditions. A frozen coefficient approximation enables its use in a variable coefficient context. Numerical results are shown to illustrate the efficiency of the preconditioner.

The Neumann-Neumann preconditioner

We consider the case of a decomposition of the plane $\mathbf{R}^2$ into two subdomains $\Omega_1 = (-\infty, 0] \times \mathbf{R}$ and $\Omega_2 = [0, \infty) \times \mathbf{R}$. The interface $\{0\} \times \mathbf{R}$ is denoted Γ. The Schur formulation is defined as follows:

Find u_0 such that the solution of the following two Dirichlet problems ($i = 1, 2$):

$$\mathcal{L}(u_i) = f \text{ in } \Omega_i, \ u_i = u_0 \text{ on } \Gamma \tag{3}$$

have matching normal derivatives on the interface Γ. Let us denote $\mathcal{S}(u_0, f) = \nu(\frac{\partial u_1}{\partial n_1} + \frac{\partial u_2}{\partial n_2})$ the jump of the normal derivatives. The Schur formulation is thus:

Find u_0 such that

$$\mathcal{S}(u_0, 0) = -\mathcal{S}(0, f). \tag{4}$$

The problem (4) once discretized is solved by a Krylov type method. Preconditioning (4) amounts to finding an approximate inverse for the operator $\mathcal{S}(., 0)$. The Neumann-Neumann preconditioner $\mathcal{T}_{NN}$ is defined as follows: let g be a function on Γ, a Neumann boundary value problem is solved in each subdomain ($i = 1, 2$)

Find v_i such that

$$\mathcal{L}(v_i) = 0 \text{ in } \Omega_i, \ \nu \frac{\partial v_i}{\partial n_i} = g \text{ on } \Gamma \tag{5}$$

The preconditioner $\mathcal{T}_{NN}$ maps g to $\frac{1}{2}(v_1 + v_2)$. By performing a Fourier transform along the interface Γ, it is possible to find the symbol of these operators (see [AN97] or [ATNV]):

$$\mathcal{S}(u_0, 0) = \mathcal{F}_\xi^{-1} \left(\sqrt{\frac{4\nu}{\Delta t} + a_x^2 + 4Ia_y\xi\nu + 4\xi^2\nu^2}\, \hat{u}_0(\xi) \right) \tag{6}$$

and

$$\mathcal{T}_{NN}(\mathcal{S}(u_0, 0)) = \mathcal{F}_\xi^{-1} \left((1 + \frac{a_x^2}{\frac{4\nu}{\Delta t} + 4Ia_y\xi\nu + 4\xi^2\nu^2})\, \hat{u}_0(\xi) \right) \tag{7}$$

where ξ is the Fourier variable, $I^2 = -1$ and $\mathcal{F}_\xi^{-1}$ denotes the inverse Fourier transform. The condition number of the discrete version of $\mathcal{TS}$ can therefore be estimated by $\frac{symbol(\mathcal{TS})(0)}{symbol(\mathcal{TS})(\infty)} = 1 + \frac{a_x^2 \Delta t}{4\nu}$. For a small time step or a very diffusive problem, the Neumann-Neumann preconditioner should perform well. For a large time step or a convection dominated flow, the condition number of $\mathcal{TS}$ can be very large.

A Robin-Robin Preconditioner

By modifying the Neumann boundary condition in (5), it is possible to have an optimal result for two semi-infinite subdomains. Indeed, let g be a function on Γ, a Robin boundary value problem is solved in each subdomain ($i = 1, 2$)

Find v_i such that

$$\mathcal{L}(v_i) = 0 \text{ in } \Omega_i, \ \nu \frac{\partial v_i}{\partial n_i} - \frac{\vec{a}.\vec{n}_i}{2} v_i = g \text{ on } \Gamma \tag{8}$$

The preconditioner $\mathcal{T}_{RR}$ maps g to $\frac{1}{2}(v_1 + v_2)$. It can be seen that (8) is well posed. By performing a Fourier transform, one sees that $\mathcal{T}_{RR}$ is an exact preconditioner, $\mathcal{T}_{RR}\mathcal{S}(., 0) = Id$.

It is interesting to note that the Robin boundary condition in (8) may arise from a variational formulation, see [ATNV]. Indeed let us consider a skew-symmetric variational formulation of (2) for some domain Ω (forgetting on purpose boundary terms):

Find u such that

$$\int_\Omega \frac{uw}{\Delta t} - \frac{1}{2} \nabla \cdot \vec{a}\, uw + \frac{1}{2}(\vec{a}.\nabla uw - \vec{a}.\nabla wu) + \nu \nabla u.\nabla w = \int_\Omega fw, \quad \forall w \tag{9}$$

Integrating by parts (9), (and this time keeping boundary terms), we get as a boundary term the Robin boundary condition in (8) :

$$\int_\Omega (\frac{u}{\Delta t} + \vec{a}.\nabla u - \nu \Delta u)w + \int_{\partial\Omega} (\nu \frac{\partial u}{\partial n} - \frac{\vec{a}.\vec{n}}{2})w = \int_\Omega fw, \quad \forall w \tag{10}$$

This remark is very useful when implementing this method in a finite element framework.
It is worth noticing that the above Robin boundary condition may also be used in a FETI context. The dual Schur formulation would consist of:

Find λ such that the solution of the following two Robin boundary value problems ($i = 1, 2$):

$$\mathcal{L}(u_i) = f \text{ in } \Omega_i, \ \nu \frac{\partial u_i}{\partial n_i} - \frac{\vec{a}.\vec{n}_i}{2} u_i = (-1)^i \lambda \text{ on } \Gamma \tag{11}$$

match on the interface Γ. Let us denote $\mathcal{DR}(\lambda, f) = \frac{1}{2}(u_2 - u_1)$ half the jump on the interface. The modified Schur formulation is thus,

Find λ such that

$$\mathcal{DR}(\lambda, 0) = -\mathcal{DR}(0, f). \tag{12}$$

The problem (12), once discretized, is solved by a Krylov type method. The optimal preconditioner is then the usual Dirichlet-Dirichlet preconditioner.

More precisely, let v be a function on Γ, a Dirichlet boundary value problem is solved in each subdomain ($i = 1, 2$)

Find v_i such that

$$\mathcal{L}(v_i) = 0 \text{ in } \Omega_i, \ v_i = v \text{ on } \Gamma \tag{13}$$

The preconditioner $\mathcal{T}_{DD}$ maps v to $\nu(\frac{\partial v_1}{\partial n_1} + \frac{\partial v_2}{\partial n_2})$. By performing a Fourier transform, one sees that $\mathcal{T}_{DD}$ is an exact preconditioner, $\mathcal{T}_{DD}\mathcal{DR}(., 0) = Id$.
Let us also mention the fact that the algorithm can be used with non matching grids on the interface and the mortar formulation see [BMP94], [Ach95], see [AN97].

An interesting feature of the Robin-Robin preconditioner is its nilpotency property for a domain decomposed into N vertical strips. Indeed, the preconditioner is then no more exact but $\mathcal{T}_{RR}\mathcal{S}(., 0) - Id$ is close to a nilpotent operator. We assume that the component of the velocity normal to the interface is positive $a_x \geq 0$. Let H denote the minimum of the widths of the subdomains. For $e^{-(a_x + \sqrt{{a_x}^2 + \frac{4\nu}{\Delta t}})H/\nu}$ small enough, the preconditioned system is close to an idempotent operator of order $\left[\frac{N}{2}\right]$ where $[x]$ denotes the integer part of x. This has an important effect on the convergence of GMRES applied to the preconditioned system since it means that a decrease of the residual should occur only after $\left[\frac{N}{2}\right]$ iterations, see Figure 1.

Theorem 1 *Assume that the velocity field $\vec{a}$ is uniform. Let $\Omega = (0, H_\Omega) \times \mathbf{R}$ be decomposed into N nonoverlapping vertical strips $\Omega_k = (l_k, l_{k+1}) \times \mathbf{R}$, $0 \leq k \leq N-1$ and $\Gamma_{k,k+1} = \{l_{k+1}\} \times \mathbf{R}$.*
Let $\mathcal{H}^s_N = \prod_{k=1}^{N-1} H^s(\Gamma_{k,k+1})$, $s \in \mathbf{R}$ be the space of H^s functions on the $N-1$ interfaces. Let $U \in \mathcal{H}^s_N$ be denoted by $U = (u_k)_{1 \leq k \leq N-1}$. The space $\mathcal{H}^s_N$ is endowed with the norm $\|U\|_{\mathcal{H}^s_{N,\infty}} = \sup_{1 \leq k \ N-1} \|u_k\|_{H^s(\Gamma_{k,k+1})}$.
Let H be the size of the smallest subdomain, $H = \min_k(l_{k+1} - l_k)$. Assume $\epsilon \equiv e^{-(a_x + \sqrt{{a_x}^2 + \frac{4\nu}{\Delta t}})H/\nu} < 1$ and that $\rho \equiv 3N\epsilon/(1-\epsilon)^{N+1} < 1$.

Then, for $n \geq \left[\frac{N}{2}\right]$, we have

$$\|(\mathcal{T} \circ \mathcal{S}(.,0) - Id)^n\|_{L(\mathcal{H}_N^s)} \leq \frac{N}{2(1-\rho)} \frac{1}{(1-\epsilon)^{N-2}} \rho^{\left[\frac{n}{\left[\frac{N}{2}\right]}\right]-1} \tag{14}$$

where $[x]$ denotes the integer part of x.

Remark 1 *In fact, as soon as $e^{(a_x - \sqrt{{a_x}^2 + \frac{4\nu}{\Delta t}})\, H/\nu} \ll 1$, $\mathcal{T} \circ \mathcal{S}$ is already very close to identity and a better estimate can easily be obtained:*

$$\|(\mathcal{T} \circ \mathcal{S}(.,0) - Id)\|_{L(\mathcal{H}_N^s)} \leq \frac{6e^{(a_x - \sqrt{{a_x}^2 + \frac{4\nu}{\Delta t}})\, H/\nu}}{(1-\epsilon)^3}. \tag{15}$$

The above theorem is thus interesting when $e^{(a_x - \sqrt{{a_x}^2 + \frac{4\nu}{\Delta t}})\, H/\nu}$ is close to 1. This corresponds for instance to the case of a very large time step with a strongly laminar flow.
On the other hand, the above results cannot be applied when the operator is symmetric and is very close to a Laplace operator ($\frac{1}{\Delta t} \ll 1$). Indeed, in order to have good convergence rates, it is then necessary to modify the Robin-Robin (which amounts to the Neumann-Neumann preconditioner) by adding a coarse space and a pseudo inverse for the Neumann problem, see [ATNV].

Numerical Results in two dimensions for the Robin-Robin preconditioner

The advection-diffusion is discretized on a Cartesian grid by a Q1-streamline-diffusion method. The system for the nodal values at the interface is solved by a preconditioned GMRES algorithm and the stopping criterion is to reduce the initial residual by a factor 10^{-10}. The preconditioners are either of the type Robin-Robin (R-R), Neumann-Neumann (N-N) or the identity (–).

A first comparison between the preconditioners

The first series of tests will be to compare the performances of the Robin-Robin (R-R), Neumann-Neumann (N-N) preconditioners, and the non-preconditioned method, in some very simple typical situations. Here, the domain is the rectangle $[0,1] \times [0,0.2]$ partitioned into five square vertical strips of sizes 0.2×0.2. In each subdomain, there is a uniform grid of 60×60 quadrangular elements. We choose $\Delta t = 1$ and $\nu = 0.001$ or $\nu = 1$, and four velocities:

1. $\vec{a} = \vec{e_1}$. In this case, the velocity is perpendicular to the interfaces between the subdomains.
2. $\vec{a} = \vec{e_2}$. In this case, the velocity is parallel to the interfaces.
3. $\vec{a} = \frac{\sqrt{2}}{2}(\vec{e_1} + \vec{e_2})$. We refer to this convecting field as *oblique*.
4. $\vec{a} = 2\pi\left((x_1 - 0.5)\vec{e_2} - (x_2 - 0.1)\vec{e_1}\right)$. Here, the convecting field can be seen as a vortex.

viscosity	Precond.\ velocity.	normal	parallel	oblique	rotating
$\nu = 0.001$	R-R	3	2	5	36
	N-N	52	2	42	> 100
	–	14	34	13	71
$\nu = 1$	R-R	9	9	10	10
	N-N	9	9	10	11
	–	30	38	41	41

Table 1: Different velocity fields and five subdomains

Based on these results, several remarks can be done:
The Robin-Robin preconditioner performs much better than the Neumann-Neumann preconditioner when the viscosity is small while the performances are equivalent for large viscosity.
For small viscosities, when the velocity is not parallel to the interface, the Neumann-Neumann preconditioner gives very poor results (poorer than when no preconditioner is used). On the contrary, when the velocity is parallel to the interfaces, both the Neumann-Neumann and the Robin-Robin preconditioners work very well (2 iterations), (note that they are equivalent in this case). These results are in complete agreement with the Fourier analysis above.
Thus, the Robin-Robin adapts smoothly to the different situations presented in the table.
In our implementation, one iteration of the Robin-Robin or Neumann-Neumann method costs twice as much as when no preconditioner is used. Even though, the Robin-Robin preconditioner remains always faster.

Influence of the number of subdomains: case of strips

The purpose of these tests is to assess the nilpotency properties of the algorithm. To illustrate the theory above, the domain is partitioned into vertical strips, the velocity is uniform and normal to the interfaces. The dependence of the number of iterations with respect to the number of strips will be investigated.

Here, the domain is $\Omega = (0, \frac{N_{sd}}{4}) \times (0, 1)$. It is partitioned into N_{sd} square subdomains, which are rectangles of sizes 0.25×1. In each subdomain, there is a uniform grid of size 20×40.

Partition		4×1	8×1	12×1	24×1	36×1
Grid		20×40	20×40	20×40	20×40	20×40
$\Delta t = 1$,	R-R	5	8	12	23	30
$\vec{a} = 3\vec{e}_1$,	–	13	18	22	33	44
$\nu = 0.001$	N-N	43	> 100	> 100	> 100	> 100

Table 2: Influence of the number of subdomains

On Figure 1(left), the convergence of the GMRES algorithms with and without the Robin-Robin preconditioner are plotted. It is very clear on Figure 1(left), that for the

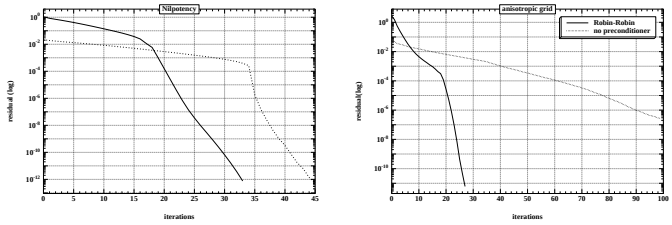

Figure 1 The convergence with and without preconditioner: 36 subdomains. Left:uniform grid. Right:anisotropic grid.

Robin-Robin preconditioner, the residual does not vary significantly for $\frac{N_{sd}}{2} = 18$ iterations, then drops quickly. This confirms very well the theory above on the idempotency of the preconditioned Schur complement matrix. For GMRES without preconditioner, the same kind of phenomenon is observed, but the decay of the residual is obtained only after $N_{sd} = 36$ iterations, see [ATNV] for details. Note that, since the number of grid nodes is not large enough, the rates of convergence after the idempotency threshold are of the same order. This would not be the case for a finer grid, as we can see Figure 1(right) and in § 1. On Figure 1(right), the convergence plots correspond to the same experiment except that the grid has been refined with a geometrical progression of ratio 0.9 in the x_2 direction. Therefore, the grid is very fine near the boundary $x_2 = 0$. We see that the idempotency properties of the preconditioned operator are conserved, although they appear less clearly. On the contrary, the non preconditioned operator yields a very poor convergence.

Influence of the grid anisotropy and boundary layers

Consider a velocity with a boundary layer near a wall

$$\begin{array}{ll} \vec{a} = 3 - (300 * (x_2 - 0.1)^2)\vec{e}_1 & \text{if } x_2 < 0.1 \\ \vec{a} = 3\vec{e}_1 & \text{if } x_2 \geq 0.1 \end{array} \tag{16}$$

To capture the boundary layer, the mesh is refined in the x_2-direction, near the wall $x_2 = 0$ with a geometric progression of ratio 0.9.

Partition		4×1	8×1	12×1	24×1	36×1
Grid		20×40	20×40	20×40	20×40	20×40
$\Delta t = 1$	R-R	11	18	25	39	51
$\nu = 0.001$	–	51	75	91	> 100	> 100
	N-N	49	> 100	> 100	> 100	> 100

Table 3 : Anisotropic grids

In comparison with the tests of § 1, we see that the performances deteriorate due to the change of velocity and grid, but is is very clear that the Robin-Robin method is the less severely affected.

Rotating velocity: influence of the number of unknowns

The domain is the unit square, which is partitioned into 4×4 subdomains. In each subdomain, the grid varies from 20×20 up to 60×60. The velocity is $\vec{a} = \vec{e_3} \times (\vec{x} - \vec{x_0})$, ($x_0$ is the center of Ω) and $\nu = 0.001$, $\Delta t = 10^7$ (almost a steady state computation). A coarse space solver of BPS type is used here, but will not be discussed.

	Partition	4×4	4×4	4×4	4×4
	Grid	20×20	30×30	40×40	60×60
$\Delta t = 10^7, \nu = 0.001$	R-R	34	34	34	34
$\vec{a} = \vec{e_3} \times (\vec{x} - \vec{x_0})$	–	80	82	89	> 100

Table 4: Influence of the number of grid points

The convergence is not affected by the grid size.

Results in three dimensions

In Table 5, we give results for a simple geometry with different partitions and velocity fields. In Table 6, the domain $[0,1] \times [0,1] \times [0,.01]$ is decomposed into 100 subdomains. The number of elements is $60,000$ and the number of nodes is $121,203$. We compare the Robin-Robin with and without coarse grid preconditioner.

Ω	$[0,1]^2 \times [0,0.5]$	$[0,1]^2 \times [0,0.33]$	$[0,1]^3$
Partition	$2 \times 2 \times 1$	$3 \times 3 \times 1$	$3 \times 3 \times 3$
$\vec{a} = (y/.5 - .5, -x/.5 + 5.0, 0)$, $\nu = 10^{-3}$, $c = 10^{-4}$			
R-R	12	21	35
N-N	24	51	165
$\vec{a} = 300 * \min(x_2^2, 0.01)\ \vec{e}_1$, $\nu = 10^{-2}$, $c = 10^{-4}$			
R-R	9	13	19
N-N	23	65	92
$\vec{a} = 3 - 300 * (\min(x_2, 0.1) - 0.1)^2\ \vec{e}_1$, $\nu = 10^{-2}$, $c = 10^{-4}$			
R-R	9	16	25
N-N	37	88	> 200

Table 5 : Iteration Count for different parameters

velocity	ν	c	R-R	R-R + coarse grid
rotating	10^{-2}	10^{-7}	51	54
null	10^{-2}	10^{-7}	78	28

Table 6: Influence of the coarse grid

Figure 2. shows the unit cube containing 24576 tetrahedric second order finite elements split into 45 subdomains by an automatic mesh partitioner. This is why the

boundaries between subdomains are less regular than for the 2D computations. For this decomposition the algorithm converges in 48 iterations with the R-R preconditioner. The last numerical example aims to be a more realistic computation : the diffusion of a pollutant in a fluid contained in a T-shape reservoir. The fluid is incompressible. For such a model if the viscosity is small, the advection is dominant, on the opposite if the viscosity increases the convection phenomena is more important than the diffusion. If, for the flow, the given initial velocity has a parabolic profile and, in the advection diffusion step, the pollutant concentration given on a boundary is linear the convection and diffusion phenomena are coupled in the hole domain, a boundary layer is expected in the large part ot the T-shape domain and a vortex region in the bottom of the domain.

The mesh considered here is too coarse to expect realistic results, it contains 29,448 elements and 43,937 nodes. The initial domain was split in 50 subdomains and the velocity field was obtained by a Stokes computation. This initial computation is in fact more expensive than the advection-diffusion one and this was the limiting point. It was performed on the same grid and same decomposition using a Neumann-Neumann domain decomposition algorithm. In this case the number of degrees of freedom is 131,811.

On this advection-diffusion problem, the Robin-Robin preconditioner converged in 81 iterations (compared to 78 iterations for an elasticity problem on the same grid). Looking at the level lines of the concentration on a transversal section (figure 3) one can see that the advection diffusion phenomena corresponds to the given boundary conditions and the vortex region appears. In addition the values are small were the boundary layer is expected. The results obtained are thus concordant with the prediction.

Optimized Schwarz algorithm

We consider in the sequel a very different type of algorithm, namely, the classical Schwarz algorithm in a simple case: the plane $\mathbf{R}^2$ is divided into two subdomains $\Omega_1 = (-\infty, \delta) \times \mathbf{R}$ and $\Omega_2 = (0, \infty) \times \mathbf{R}$. Numerical results will be given for general decompositions. The size of the overlap is $\delta \geq 0$. In order to solve (2), the classical additive Schwarz method is based on the use of Dirichlet boundary conditions

$$\mathcal{L}(u_i^{k+1}) = f \text{ in } \Omega_i, u_i^{k+1} = u_{3-i}^k. \tag{17}$$

A Fourier analysis shows that

$$\hat{u}(x,\xi) - \hat{u}_i^{k+1}(x,\xi) = e^{-\sqrt{\frac{4\nu}{\Delta t/\nu} + a_x^2 + 4Ia_y\xi\nu + 4\xi^2\nu^2}\delta}(\hat{u}(x,\xi) - \hat{u}_i^{k-1}(x,\xi)) \tag{18}$$

and overlap is necessary for convergence. For a small overlap ($\delta \ll 1$), the convergence will be very slow. In order to remedy to this situation, it has been proposed to use more general interface conditions. The algorithm reads

$$\mathcal{L}(u_i^{k+1}) = f \text{ in } \Omega_i, \mathcal{B}_i(u_i^{k+1}) = \mathcal{B}_i(u_{3-i}^k). \tag{19}$$

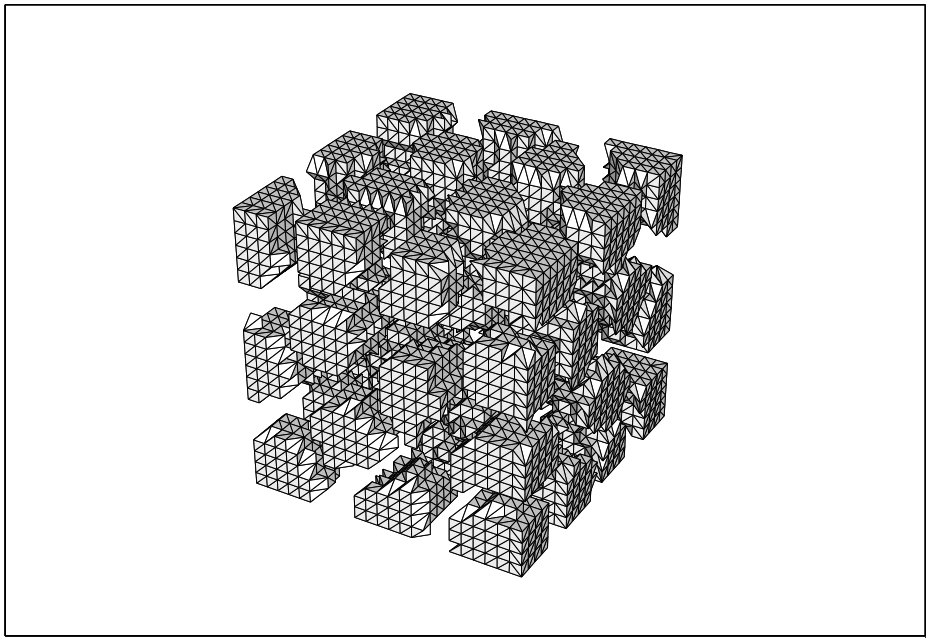

Figure 2 Three dimensional triangulation and automatic decomposition into 45 subdomains

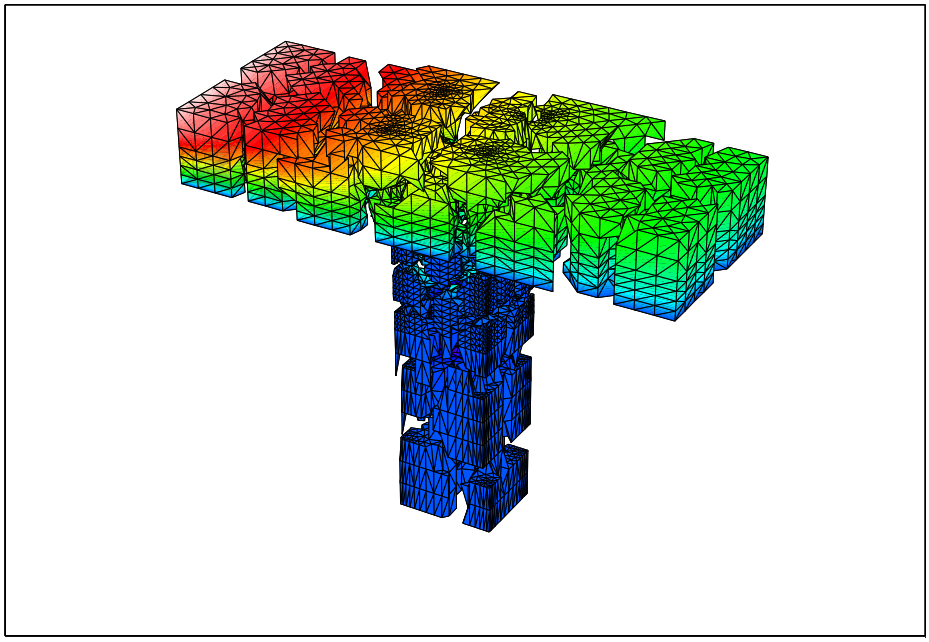

Figure 3 Three dimensional triangulation and automatic decomposition into 50 subdomains

where $\mathcal{B}_i(u) = \nu \frac{\partial u}{n_i} - \mathcal{F}_\xi^{-1}(\lambda_i(\xi)\hat{u}(x,\xi))$. A Fourier analysis shows that (see [NR94])

$$\hat{u}(x,\xi) - \hat{u}_i^{k+1}(x,\xi) = \frac{\lambda_1^e(\xi) - \lambda_1(\xi)}{\lambda_2^e(\xi) + \lambda_1(\xi)} \frac{\lambda_2^e(\xi) - \lambda_2(\xi)}{\lambda_1^e(\xi) + \lambda_2(\xi)} \tag{20}$$

$$\times\ e^{-\sqrt{\frac{4\nu}{\Delta t} + a_x^2 + 4Ia_y\xi\nu + 4\xi^2\nu^2}\delta/\nu} (\hat{u}(x,\xi) - \hat{u}_i^{k-1}(x,\xi)) \tag{21}$$

where

$$\lambda_1^e(\xi) = \frac{a_x + \sqrt{\frac{4\nu}{\Delta t} + a_x^2 + 4Ia_y\xi\nu + 4\xi^2\nu^2}}{2}, \tag{22}$$

$$\lambda_2^e(\xi) = \frac{-a_x + \sqrt{\frac{4\nu}{\Delta t} + a_x^2 + 4Ia_y\xi\nu + 4\xi^2\nu^2}}{2}. \tag{23}$$

If $\lambda_i = \lambda_i^e$, we have convergence in two steps (see [HTJ88] or [FNdS94]). These optimal interface conditions are also exact absorbing boundary conditions which are used for truncating infinite domains. The fact that these interface conditions are optimal for domain decomposition methods is quite general since it applies to variable coefficient operators and more general decompositions as well, see [FNdS94]. In the case of the Laplace operator, their use had also been suggested in [Lio90]. Because of the square root in formulas (22) and (23), these boundary operators are not not differential operators. They are of integro-differential (or pseudo-differential) type and thus difficult to implement numerically. As it is the case when they are used for truncating infinite domains, they are approximated by partial differential operators. In [DJR92], and then in [Des93], [BD97], [GGQ96] [dLBFM+98], [MSRKA98] and [CCEW98], the lowest order approximations used for the truncation of domains are used as interface conditions for domain decomposition domains. It amounts to taking $\lambda_i = \lambda_i^e(0)$ (*Taylor approximation at order 0*). In [NR94] higher order approximations are used for the convection-diffusion equation, namely *Taylor approximation at order 2* of $\lambda_i^e(\xi)$ in the vicinity of $\xi = 0$.

Optimized of Order 2 (OO2) Interface Conditions

A more suited and efficient possibility is to optimize the choice of the interface conditions $\mathcal{B}_i$ with respect to the convergence of the domain decomposition method (see [TB94], [EZ98] for the operator $\eta - \Delta$, and [Jap97] for the convection-diffusion equation and [CN98] for the wave equation). For ease of implementation, $\mathcal{B}_i$ is sought in the form

$$\mathcal{B}_i = \nu \frac{\partial}{\partial n_i} + \alpha_i + \beta_i \frac{\partial}{\partial \tau_i} - \gamma_i \frac{\partial^2}{\partial \tau_i^2}. \tag{24}$$

The parameters are chosen in order to minimize the maximum of the convergence rate over all the wavenumbers which can be represented on the computational grid, $|\xi| \leq 1/h$ (h is the typical mesh size):

$$\min_{\alpha_1,\beta_1,\gamma_1,\alpha_2,\beta_2,\gamma_2} \max_{|\xi| \leq 1/h} \rho(\xi, \alpha_1, \beta_1, \gamma_1, \alpha_2, \beta_2, \gamma_2) \tag{25}$$

where

$$\rho(\xi,\alpha_1,\beta_1,\gamma_1,\alpha_2,\beta_2,\gamma_2) = \left|\frac{\lambda_1^e(\xi)-(\alpha_1+\beta_1 I\xi+\gamma_1\xi^2)}{\lambda_2^e(\xi)+(\alpha_1+\beta_1 I\xi+\gamma_1\xi^2)}\right| \times \left|\frac{\lambda_2^e(\xi)-(\alpha_2-\beta_2 I\xi+\gamma_2\xi^2)}{\lambda_1^e(\xi)+(\alpha_2-\beta_2 I\xi+\gamma_2\xi^2}\; e^{-\sqrt{\frac{4\nu}{\Delta t}+a_x^2+4Ia_y\xi\nu+4\xi^2\nu^2}\delta/\nu}\right| \tag{26}$$

This minimization problem is difficult since it is not differentiable nor convex. It can be proved that choosing $\alpha_i,\gamma_i \geq 0$, $\alpha_2-\alpha_1 = a_x$, $\beta_1 = -\beta_2$, $\gamma_1 = \gamma_2$ and $sgn(\beta_1) = -sgn(\beta_2) = sgn(a_y)$ is sufficient for having $|\rho| < 1$. Moreover, when $a_y = 0$, the min-max problem (25) is equivalent to a 1D minimization problem over a wavenumber ξ_{int} such that $\rho(\xi_{int}) = 0$. In the general case $a_y \neq 0$ this last procedure is used, see [Jap97]. In the limit $h \to 0$, a theoretical estimate shows that for the Taylor interface conditions at order 0 or 2 , $\rho \simeq 1 - C^t|a|h/\nu$ while for the OO2 interface condition $\rho \simeq 1 - C^t(|a|h/\nu)^{1/3}$. For a variable coefficient operator, a frozen coefficient approximation is used for computing the parameters of the interface condition.
In order to improve the convergence, the iterative algorithm (19) is replaced by a Krylov type method applied to the substructured problem with $\mathcal{B}_i(u)$ as unknowns on the interfaces, see [NR94].

Numerical Results for the OO2 method

Dirichlet, Taylor of order zero, Taylor of order 2 and OO2 interface conditions are compared. A BICGSTAB algorithm is used for the substructured problem. The stopping criterion was the maximum error between the converged solution and the iterative solution to be smaller than 10^{-6}. The problems in the subdomains are solved by a direct method.
We first consider an upwind finite difference scheme with a small overlap of size h. The time step is taken very large ($\Delta t = 10^9$) so that it corresponds to a stationary equation. For a decomposition into 16×1 subdomains, we have the following iteration count for two velocity fields: one normal to the interface and one tangential to the interface:

Nb of iterations	**Dirichlet**	**Taylor 0**	**Taylor 2**	**002**
$a_y = 0,\ a_x = y$	60	137	15	15
$a_x = 0,\ a_y = x$	60	90	265	9

Table 5: Overlapping subdomains - $\nu = 10^{-2}$, $h = 1/241$

We see that the OO2 interface conditions lead to the fastest algorithms.
We now consider a finite volume discretization with no overlap between the subdomains ($\delta = 0$). The Dirichlet interface conditions cannot be used anymore. For the same parameters as in Table 5, we have

Nb of iterations	**Taylor 0**	**Taylor 2**	**002**
$a_y = 0,\ a_x = y$	140	122	18
$a_x = 0,\ a_y = x$	85	divergence	20

Table 6: Non Overlapping subdomains - $\nu = 10^{-2}$, $h = 1/241$

Once more, the OO2 interface conditions give the best results. We now focus on the robustness of the algorithms which are illustrated by the following tables. These results can be related to the estimate of § 1.

Nb of points	65×65	129×129	241×241
OO2	25	26	30
Taylor 0	76	130	224

Table 7: Non Overlapping subdomains– **4** by **4** subdomains–rotating velocity field

$\|a\|\Delta t/h$	10^0	10^3	10^5	10^9
OO2	3	12	15	15
Taylor 0	3	18	48	141
Taylor 2	2	21	58	123

Table 8 Non Overlapping subdomains– **16** by **1** subdomains – boundary layer velocity field

When the operator degenerates to a Laplace operator, a coarse grid preconditioner has to be used in order to keep the robustness of the method, see [JNR98].

Conclusion

We have presented two very different methods which are adapted to non symmetric scalar problems. It seems to us that they perform essentially equally well (see Tables 4 and 7) although a thorough study should be made. Through its variational formulation (see (10), the Robin-Robin preconditioner can be easily implemented in a FEM. As for the OO2 approach, its extension to other type of equations seems more easily feasible. An interesting perspective is the extension of both approaches to systems of equations.

REFERENCES

[Ach95] Achdou Y. (1995) The mortar element method for convection diffusion problems. *C. R. Acad. Sci. Paris Sér. I Math.* 321(1): 117–123.

[AN97] Achdou Y. and Nataf F. (1997) A robin-robin preconditioner for an advection-diffusion problem. *C.R. Acad. Sci. Série I* 325: 1211–1216.

[ATNV] Achdou Y., Tallec P. L., Nataf F., and Vidrascu M.A domain decomposition preconditioner for an advection-diffusion problem. to apper.

[BD97] Benamou J.-D. and Després B. (1997) A domain decomposition method for the Helmholtz equation and related optimal control problems. *J. Comput. Phys.* 136(1): 68–82.

[BGLTV89] Bourgat J.-F., Glowinski R., Le Tallec P., and Vidrascu M. (1989) Variational formulation and algorithm for trace operator in domain decomposition calculations. In Chan T., Glowinski R., Périaux J., and Widlund O. (eds) *Domain Decomposition Methods*, pages 3–16. SIAM, Philadelphia, PA.

[BMP94] Bernardi C., Maday Y., and Patera A. T. (1994) A new non conforming approach to domain decomposition: The mortar element method. In Brezis H. and Lions J.-L. (eds) *Collège de France Seminar*. Pitman. This paper appeared as a technical report about five years earlier.

[CCEW98] Cai X.-C., Casarin M. A., Elliott Frank W. J., and Widlund O. B. (1998) Overlapping Schwarz algorithms for solving Helmholtz's equation. In *Domain decomposition methods, 10 (Boulder, CO, 1997)*, pages 391–399. Amer. Math. Soc., Providence, RI.

[CN98] Chevalier P. and Nataf F. (1998) Symmetrized method with optimized second-order conditions for the Helmholtz equation. In *Domain decomposition methods, 10 (Boulder, CO, 1997)*, pages 400–407. Amer. Math. Soc., Providence, RI.

[Des93] Després B. (1993) Domain decomposition method and the Helmholtz problem. II. In *Second International Conference on Mathematical and Numerical Aspects of Wave Propagation (Newark, DE, 1993)*, pages 197–206. SIAM, Philadelphia, PA.

[DJR92] Després B., Joly P., and Roberts J. E. (1992) A domain decomposition method for the harmonic Maxwell equations. In *Iterative methods in linear algebra (Brussels, 1991)*, pages 475–484. North-Holland, Amsterdam.

[dLBFM+98] de La Bourdonnaye A., Farhat C., Macedo A., Magoulès F., and Roux F.-X. (1998) A non-overlapping domain decomposition method for exterior Helmholtz problem. In *Domain decomposition methods, 10 (Boulder, CO, 1997)*, pages 42–66. Amer. Math. Soc., Providence, RI.

[EZ98] Engquist B. and Zhao H.-K. (1998) Absorbing boundary conditions for domain decomposition. *Appl. Numer. Math.* 27(4): 341–365. Absorbing boundary conditions.

[FMR94] Farhat C., Mandel J., and Roux F.-X. (1994) Optimal convergence properties of the FETI domain decomposition method. *Comput. Methods Appl. Mech. Engrg.* 115(3-4): 365–385.

[FNdS94] F. Nataf F. R. and de Sturler E. (1994) Optimal interface conditions for domain decomposition methods. Technical Report 301, CMAP (Ecole Polytechnique).

[GGQ96] Gastaldi F., Gastaldi L., and Quarteroni A. (1996) Adaptive domain decomposition methods for advection dominated equations. *East-West J. Numer. Math.* 4(3): 165–206.

[HTJ88] Hagstrom T., Tewarson R. P., and Jazcilevich A. (1988) Numerical experiments on a domain decomposition algorithm for nonlinear elliptic boundary value problems. *Appl. Math. Lett.* 1(3): 299–302.

[Jap97] Japhet C. (1997) Conditions aux limites artificielles et décomposition de domaine: Méthode oo2 (optimisé d'ordre 2). application à la résolution de problèmes en mécanique des fluides. Technical Report 373, CMAP (Ecole Polytechnique).

[JNR98] Japhet C., Nataf F., and Roux F.-X. (1998) Extension of a coarse grid preconditioner to non-symmetric problems. In *Domain decomposition methods, 10 (Boulder, CO, 1997)*, pages 279–286. Amer. Math. Soc., Providence, RI.

[Lio90] Lions P. L. (1990) On the Schwarz alternating method. III: a variant for nonoverlapping subdomains. In Chan T. F., Glowinski R., Périaux J., and Widlund O. (eds) *Third International Symposium on Domain Decomposition Methods for Partial Differential Equations , held in Houston, Texas, March 20-22, 1989*. SIAM, Philadelphia, PA.

[MSRKA98] McInnes L. C., Susan-Resiga R. F., Keyes D. E., and Atassi H. M. (1998) Additive Schwarz methods with nonreflecting boundary conditions for the parallel computation of Helmholtz problems. In *Domain decomposition methods, 10 (Boulder, CO, 1997)*, pages 325–333. Amer. Math. Soc., Providence, RI.

[NR94] Nataf F. and Rogier F. (1994) Outflow boundary conditions and domain decomposition method. In *Domain decomposition methods in scientific and engineering computing (University Park, PA, 1993)*, pages 289–293. Amer. Math. Soc., Providence, RI.

[TB94] Tan K. H. and Borsboom M. J. A. (1994) On generalized Schwarz coupling applied to advection-dominated problems. In *Domain decomposition methods in scientific and engineering computing (University Park, PA, 1993)*, pages 125–130. Amer. Math. Soc., Providence, RI.